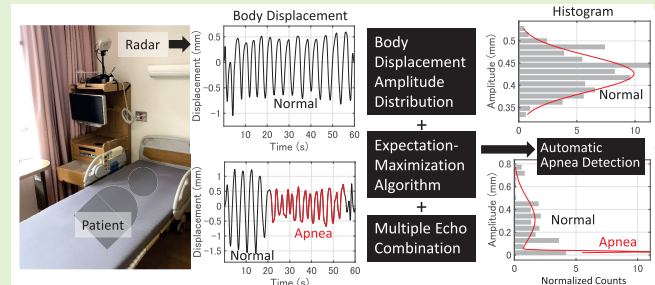


Noncontact Detection of Sleep Apnea Using Radar and Expectation–Maximization Algorithm

Takato Koda^{ID}, Shigeaki Okumura, Hirofumi Taki, *Member, IEEE*, Satoshi Hamada, Hironobu Sunadome, Susumu Sato, Kazuo Chin, and Takuya Sakamoto^{ID}, *Senior Member, IEEE*

Abstract—Sleep apnea syndrome (SAS) requires early diagnosis because this syndrome can lead to a variety of health problems. If sleep apnea (SA) events can be detected in a noncontact manner using radar, we can then avoid the discomfort caused by the contact-type sensors that are used in conventional polysomnography (PSG). This study proposes a novel radar-based method for accurate detection of SA events. The proposed method uses the expectation–maximization (EM) algorithm to extract the respiratory features that form normal and abnormal breathing patterns, resulting in an adaptive apnea detection capability without any requirement for empirical parameters. We conducted an experimental quantitative evaluation of the proposed method by performing PSG and radar measurements simultaneously in five patients with the symptoms of SAS. Through these experiments, we show that the proposed method can detect the number of apnea and hypopnea events per hour with an error of 4.8 times/h; this represents an improvement in the accuracy by 1.8 times when compared with the conventional threshold-based method and demonstrates the effectiveness of our proposed method.

Index Terms—Antenna arrays, biomedical engineering, Doppler radar, radar measurements, radar signal processing.



I. INTRODUCTION

THE number of adults aged from 30 to 69 years that display moderate to severe symptoms of sleep apnea

Manuscript received 9 July 2024; revised 22 August 2024; accepted 24 August 2024. Date of publication 9 September 2024; date of current version 16 October 2024. This work was supported in part by Japan Science and Technology Agency under Grant JPMJPR1873, Grant JPMJCE1307, Grant JPMJMI22J2, and Grant JPMJMS2296; in part by the SECOM Science and Technology Foundation; and in part by Japan Society for the Promotion of Science KAKENHI under Grant 19H02155, Grant 21H03427, Grant 23H01420, and Grant 23K26115. The associate editor coordinating the review of this article and approving it for publication was Prof. Pierluigi Salvo Rossi. (Corresponding author: Takuya Sakamoto.)

This work involved human subjects or animals in its research. Approval of all ethical and experimental procedures and protocols was granted by the Kyoto University, Graduate School of Medicine's Ethics Committee under Application No. R2042.

Takato Koda and Takuya Sakamoto are with the Graduate School of Engineering, Kyoto University, Kyoto 615-8510, Japan (e-mail: sakamoto.takuya.8n@kyoto-u.ac.jp).

Shigeaki Okumura and Hirofumi Taki are with MaRI Company Ltd., Kyoto 600-8815, Japan (e-mail: sokumura@marisleep.co.jp; taki@marisleep.co.jp).

Satoshi Hamada, Hironobu Sunadome, and Susumu Sato are with the Graduate School of Medicine, Kyoto University, Kyoto 606-8501, Japan (e-mail: sh1124@kuhp.kyoto-u.ac.jp; sankichi@kuhp.kyoto-u.ac.jp; ssato@kuhp.kyoto-u.ac.jp).

Kazuo Chin is with the Graduate School of Medicine, Kyoto University, Kyoto 606-8501, Japan, and also with the School of Medicine, Nihon University, Itabashi-ku, Tokyo 173-8610, Japan (e-mail: chin.kazuo@nihon-u.ac.jp).

Digital Object Identifier 10.1109/JSEN.2024.3450890

syndrome (SAS) is estimated to be approximately 425 million worldwide [1], [2]. SAS is known to increase the risk of complications, such as hypertension, coronary artery disease, and cerebrovascular disease and can also lead to work-related errors and traffic accidents because of daytime sleepiness and poor concentration [3]. To avoid these risks, early diagnosis and treatment are essential [4], [5], and the gold standard for SAS testing is polysomnography (PSG) [6]. PSG records various physiological signals, including electroencephalography (EEG), electrocardiography (ECG), and arterial blood oxygen saturation signals throughout the night using contact-type sensors. When compared with the conventional PSG technique, radar-based noncontact SAS monitoring offers the advantage that the discomfort caused to the patient by contact-type sensors can be avoided, thus enabling monitoring of the SAS signs during natural sleep.

Many existing studies of noncontact detection of sleep apnea (SA) are based on machine learning (ML) methods [7], [8], [9], [10], [11], [12], [13], [14], including long short-term memory (LSTM) [9], [13], [14] and support vector machine (SVM) techniques [8], [10], [11]. Although ML-based methods often require sufficient quantities of training data to be available for accurate classification, it is not easy to collect enough data effectively because the radar data depend on the measurement setup and the surrounding environment and also depend on the positioning and angle of the radar system [9], [13], thus limiting the use of ML in practice.

In contrast, test methods without the use of ML have also been reported [15], [16], [17], [18], [19], [20], [21], [22], [23], [24], [25], and some of these methods are based on thresholding in terms of the displacement amplitude. For example, in a study by Kagawa et al. [19], [20], a threshold was set up using the amplitude of the displacement caused by normal respiration. Another example is a study by Kang et al. [25] that proposed a method for the use of adaptive thresholding in a constant false alarm rate (CFAR) framework. These methods require prior information about the normal respiration of the target patient, which limits the practicality of the methods.

Unlike conventional ML-based or threshold-based methods, this study introduces a new approach that uses the statistical distribution of respiratory displacement. The proposed method uses the expectation–maximization (EM) algorithm to estimate parameters for stochastic models of respiratory displacement and distinguish between normal breathing and apnea to detect apnea without using numerous training datasets or threshold values. In this study, we conducted experiments on five patients who had been hospitalized for SA testing using PSG and evaluated the accuracy of apnea event detection using the proposed method. Through these experiments, we demonstrate that the proposed method can detect apnea events with higher accuracy than the conventional threshold-based method.

II. SA DETECTION USING ARRAY RADAR

A. Millimeter-Wave Array Radar

In this study, we apply a millimeter-wave radar system that uses the frequency-modulated continuous-wave (FMCW) method with a center frequency of 79 GHz, a center wavelength of $\lambda = 3.8$ mm, range resolution of 43 mm, transmit power of 9 dBm, an equivalent isotropic radiated power of 20 dBm, and a slow-time sampling frequency of 10 Hz. The antennas of this radar system comprise a multiple-input multiple-output (MIMO) array that contains three transmitting elements and four receiving elements, corresponding to a 12-element virtual array; the transmitting and receiving arrays are linear arrays that are equally spaced at intervals of 2λ (7.6 mm) and $\lambda/2$ (1.9 mm), respectively. The radiation pattern for each element is defined as $\pm 4^\circ$ and $\pm 35^\circ$ in the E - and H -planes, respectively. The three transmitting elements radiate signals one-by-one in a time-division multiplexing manner.

B. Radar Imaging and Extraction of Respiratory Displacements

The FMCW radar system transmits a linear chirp signal with a constant amplitude and a frequency $f_T(\tau)$ that increases linearly, as described by $f_T(\tau) = f_0 + B\tau/T_0$ over the interval $0 \leq \tau \leq T_0$, where τ is a fast time, f_0 is the initial frequency, B is the bandwidth, and T_0 is the chirp duration. The echo reflected from a target located at a distance r from the radar system can be approximated using a time-delayed attenuated copy of the transmitted signal, and the echo frequency $f_R(\tau)$ can thus be expressed as $f_R(\tau) = f_0 + B(\tau - 2r/c)/T_0$, where c is the speed of light. The transmitted and received signals are then input into a mixer with a low-pass filter to generate an intermediate-frequency (IF) signal with a frequency f_{IF} , which is a beat frequency and is given by

$f_{IF} = f_T(\tau) - f_R(\tau) = 2Br/cT_0$. Therefore, to estimate the target range $r = (cT_0/2B)f_{IF}$, the Fourier transform of the IF signal is calculated to estimate the signal frequency f_{IF} , where the Fourier transform is often implemented using the fast Fourier transform algorithm.

By applying a Fourier transform to the FMCW radar data with regard to the fast time, we obtain a signal $s'_k(t, r)$, where t is the slow time, r is the range, and $k(=0, 1, \dots, K-1)$ is the element number of the virtual array, with the number of virtual elements being denoted by $K = 12$. Note that the phase of the signal $s'_k(t, r)$ was assumed to be calibrated in advance.

By assuming that the k th virtual array element is located at $(x, y) = (x_k, 0)$ in the xy plane, where $x_k = k\lambda/2$, the signal vector $s(t, r)$ can then be obtained as follows:

$$s(t, r) = [s_0(t, r), s_1(t, r), \dots, s_{K-1}(t, r)]^T \quad (1)$$

where $s_k(t, r) = c_k s'_k(t, r)$, c_k is a Taylor window coefficient and the superscript T denotes a matrix/vector transpose operator. Using the beamformer weight vector $w(\theta) = [w_0, w_1, \dots, w_{K-1}]^T$ along with $w_k(\theta) = e^{-j(2\pi x_k/\lambda) \sin \theta} = e^{-j\pi k \sin \theta}$ ($k = 0, 1, \dots, K-1$), a complex-valued radar image $I_0(t, r, \theta) = w^H(\theta)s(t, r)$ is then generated, where H denotes the complex conjugate transpose operator.

We then suppress the static clutter components as follows:

$$I_c(t, r, \theta) = I_0(t, r, \theta) - \frac{1}{T_c} \int_{t-T_c}^t I_0(\tau, r, \theta) d\tau \quad (2)$$

where $I_c(t, r, \theta)$ is a clutter-free complex-valued radar image and T_c is a time period. Because the static clutter components are echoes from nontarget stationary objects, e.g., desks, chairs, and walls, they are not dependent on the slow time t within the time period T_c , which means that the static clutter can be estimated by averaging the radar image $I_0(t, r, \theta)$ with respect to t . In this study, we selected the average time length $T_c = 30$ s empirically [26]. We should note here that if the clutter is neither homogeneous nor stationary, other approaches, e.g., circle fitting, must be used to suppress the clutter.

If the signal received contains only a single dominant echo from the target human body, which is located at (r_0, θ_0) , then the signal received from an angle θ_0 is approximated to be proportional to the phase-modulated term; i.e., $I_c(t, r, \theta_0) \propto e^{j4\pi d_0(t)/\lambda}$ with an echo waveform $p(t, r)$, and the body displacement $d_0(t)$ is thus obtained as follows:

$$d_0(t) = \frac{\lambda}{4\pi} \angle I_c(t, r_0, \theta_0) \quad (3)$$

where \angle represents the phase of a complex number. The respiratory displacement $d(t)$ is estimated using a bandpass filter to suppress the body motion and the random noise components. The cutoff frequencies of the filter are set at 0.17 and 1.8 Hz, corresponding to 0.55 and 6 s in the time domain, respectively.

C. Limitations of the Conventional Apnea Detection Method

According to the American Academy of Sleep Medicine (AASM) scoring criteria for SAS, ventilation is reduced by

30% when compared with normal breathing during hypopnea and by more than 90% during apnea [1], [2], [27], [28], [29], [30], and any such events that last longer than 10 s are counted as hypopnea or apnea, respectively [27], [28]. Therefore, the body motion caused by respiration is reduced during hypopnea and apnea events, and many conventional methods detect this reduced body motion. One such example is the amplitude baseline method (ABM) [19], [20], which is referred to as the conventional method for the purposes of performance comparison in this study.

The displacement amplitude $\bar{d}(t)$ is given by

$$\bar{d}(t) = \sqrt{\frac{1}{T_a} \int_{t-T_a/2}^{t+T_a/2} |d(\tau)|^2 d\tau} \quad (4)$$

where we set $T_a = 5$ s because the typical respiratory interval is usually shorter than 5 s. The ABM first estimates the body displacement amplitude \bar{d}_b during normal breathing to act as a baseline and then sets a threshold $\beta \bar{d}_b$ to detect reduced displacement. Based on consideration of the AASM criteria, the threshold value is set at either 70% or 50% ($\beta = 0.7$ or 0.5) of the amplitude for normal breathing \bar{d}_b . The ABM detects the apnea and hypopnea event period $[t_1, t_2]$, where $\bar{d}(t) < \beta \bar{d}_b$ holds for any value of t that satisfies the relation $t_1 \leq t \leq t_2$. In addition, the condition $t_2 - t_1 \geq T_m = 10$ s must be satisfied according to the AASM criteria.

The limitation of the ABM lies in the fact that normal breathing must first be detected as a baseline, which is not always easy in practice. In addition, the accuracy of the ABM decreases when the patient's position and posture change, which is the reason why a new method is proposed in Section III.

III. PROPOSED APNEA DETECTION METHOD

A. Respiratory Features Extraction With EM Algorithm

We propose a method that uses the EM algorithm for apnea detection. In this method, we regard the respiratory displacement amplitude \bar{d} as a random variable and assume that \bar{d} follows a Gaussian distribution with a mean μ_1 and a variance Σ_1 during apnea and hypopnea events; in addition, we assume that \bar{d} also follows a Gaussian distribution with a mean μ_2 and a variance Σ_2 during normal breathing periods. The respiratory displacement amplitude, including both the apnea and normal breathing, can then be expressed as a Gaussian mixture model.

First, we define the mixing ratios π_1 and π_2 ($\pi_1 + \pi_2 = 1$), which represent the ratios of the time lengths of apnea and normal breathing. Using the vectors $\boldsymbol{\mu} = [\mu_1, \mu_2]^T$, $\boldsymbol{\Sigma} = [\Sigma_1, \Sigma_2]^T$, and $\boldsymbol{\pi} = [\pi_1, \pi_2]^T$, the probability density function $G(\bar{d}|\boldsymbol{\pi}, \boldsymbol{\mu}, \boldsymbol{\Sigma})$ of \bar{d} is given by

$$G(\bar{d}|\boldsymbol{\pi}, \boldsymbol{\mu}, \boldsymbol{\Sigma}) = \sum_{k=1}^{K_e} \pi_k \mathcal{N}(\bar{d}|\mu_k, \Sigma_k) \quad (5)$$

where $\mathcal{N}(\cdot|\mu, \Sigma)$ is the probability density function of a normal distribution with a mean μ and a variance Σ , and the number of mixture components K_e is set to be $K_e = 2$.

If we assume that \bar{d} is observed M times (i.e., \bar{d}_i ($i = 1, 2, \dots, M$)), then the log-likelihood function $L(\bar{d}_i|\boldsymbol{\pi}, \boldsymbol{\mu}, \boldsymbol{\Sigma})$

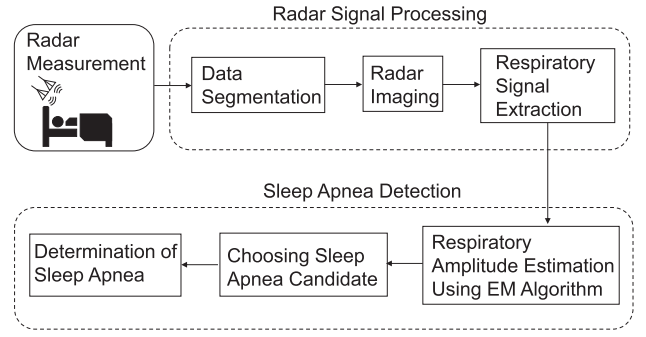


Fig. 1. Overview of the proposed apnea detection method.

is given as follows:

$$L(\bar{d}_i|\boldsymbol{\pi}, \boldsymbol{\mu}, \boldsymbol{\Sigma}) = \log \prod_{i=1}^M G(\bar{d}_i|\boldsymbol{\pi}, \boldsymbol{\mu}, \boldsymbol{\Sigma}) \\ = \sum_{i=1}^M \log \left[\sum_{k=1}^{K_e} \pi_k \mathcal{N}(\bar{d}_i|\mu_k, \Sigma_k) \right]. \quad (6)$$

To determine the parameters $\boldsymbol{\mu}$ and $\boldsymbol{\pi}$, we use the EM algorithm, which consists of an expectation (E) step that calculates the posterior probability over the hidden variable $\gamma_{k,i}$ using the current parameters π_k , μ_k , and Σ_k , and a maximization (M) step that estimates the parameters π_k , μ_k , and Σ_k using the current value of $\gamma_{k,i}$. Here, $z_{i,k}$ denotes the probability that the i th data sample \bar{d}_i is generated by the k th Gaussian distribution $\pi_k \mathcal{N}(\bar{d}|\mu_k, \Sigma_k)$. $\gamma_{k,i}$ is estimated as follows:

$$\gamma_{k,i} = \frac{\pi_k \mathcal{N}(\bar{d}_i|\mu_k, \Sigma_k)}{\sum_{k=1}^{K_e} \pi_k \mathcal{N}(\bar{d}_i|\mu_k, \Sigma_k)}. \quad (7)$$

The optimal parameters π_k^* , μ_k^* , and Σ_k^* are given by

$$\pi_k^* = \frac{M_k}{M} \quad (8)$$

$$\mu_k^* = \frac{1}{M_k} \sum_{i=1}^M \gamma_{k,i} \bar{d}_i \quad (9)$$

$$\Sigma_k^* = \frac{1}{M_k} \sum_{i=1}^M \gamma_{k,i} (\bar{d}_i - \mu_k^*)^2 \quad (10)$$

where $M_k = \sum_{i=1}^M \gamma_{k,i}$.

B. Proposed Apnea Detection Method

We propose a radar-based system for apnea detection, as illustrated in Fig. 1. The proposed system consists of a radar signal processing block and an SA detection block.

First, the overnight radar signal data are divided into epochs, with each having a period of $T_{ep} = 60$ s, where the adjacent epochs overlap by 30 s following the convention of the PSG test procedures. Next, the radar image $I_p(r, \theta)$ is generated as follows:

$$I_p(r, \theta) = \frac{1}{T_{ep}} \int_0^{T_{ep}} |I_c(t, r, \theta)|^2 dt. \quad (11)$$

From the radar image $I_p(r, \theta)$, local maxima with intensities greater than a specific threshold are extracted, and their range

and azimuth characteristics are obtained from (r_m, θ_m) ($m = 1, 2, \dots, M$), which correspond to multiple scattering centers on the human body. From the results for the positions (r_m, θ_m) , we obtain a respiratory displacement $d_m(t)$ and an amplitude $\bar{d}_m(t)$ using (3) and (4). The proposed method uses the displacement waveform not only at a single scattering center but also at multiple scattering centers across the human body because the apnea and hypopnea movements vary depending on the body part involved [28]. By applying the EM algorithm to the displacement amplitude $\bar{d}_m(t)$, the parameters $\pi_{k,m}$, $\mu_{k,m}$, and $\Sigma_{k,m}$ ($k = 1, 2$) are estimated, where $\mu_{1,m} \leq \mu_{2,m}$.

Let us define a label $l_m(t)$ as $l_m(t) = 1$ if an apnea and hypopnea event is detected from the m th displacement amplitude at a time t , and let $l_m(t) = 0$ otherwise. The proposed method estimates this label as follows:

$$l_m(t) = \begin{cases} 1, & \text{if } \gamma_{1,m}(t) \leq \gamma_{2,m}(t), \text{ and } \frac{\mu_{1,m}}{\mu_{2,m}} \leq \beta \\ 0, & \text{otherwise.} \end{cases} \quad (12)$$

Here, we set $\beta = 0.5$ based on the AASM scoring criteria that were established in 1999 [2], [27], [28]. In (12), the presence or absence of apnea and hypopnea events is determined by the ratio of $\mu_{1,m}$ to $\mu_{2,m}$. Finally, we make our decision by using all $l_m(t)$ ($m = 1, \dots, M$) as shown

$$l(t) = \begin{cases} 1, & \text{if } \sum_{m=1}^M l_m(t) \mu_{2,m} > \sum_{m=1}^M \mu_{2,m} / 2 \\ 0, & \text{otherwise.} \end{cases} \quad (13)$$

This approach detects the presence of an apnea and hypopnea event if that apnea and hypopnea event is detected at the majority of the patient's body parts in the radar signals. Because each epoch has a 50% overlap with its neighboring epoch, the sum of the labels $l(t)$ for each of the apnea events must be either 0, 1, or 2. Therefore, the proposed method only detects the presence of an apnea and hypopnea event when this sum value reaches 2 and the event lasts for more than 10 s.

IV. EXPERIMENTAL PERFORMANCE EVALUATION

A. Overview of the Experimental Setup

To evaluate the performance of the proposed method, we performed radar measurements on patients with SAS symptoms, where the radar and PSG measurements were performed simultaneously, and an evaluation was also performed using conventional medical diagnostic results. The details of the five participating patients with minor to moderate SAS symptoms are presented in Table I. Fig. 2 shows the measurement setup with the radar system in a hospital room. Because we are interested in apnea and hypopnea events in this work, we only analyzed the radar data acquired when the patients were asleep. The awakeness of each patient was detected using the PSG data. In Section IV-B, we apply the proposed method to the radar data and compare the results with the PSG data to evaluate the method's performance.

B. Application of the Proposed Method

In this section, we apply the proposed method to the experimental data to evaluate the method's performance. Fig. 3



Fig. 2. Measurement setup with millimeter-wave array radar system in a hospital room.

TABLE I
PATIENT DETAILS

Patient number	Radar measurement time (h)	Number of apnea events
1	7.0	104
2	6.5	154
3	5.5	68
4	7.0	25
5	8.0	117

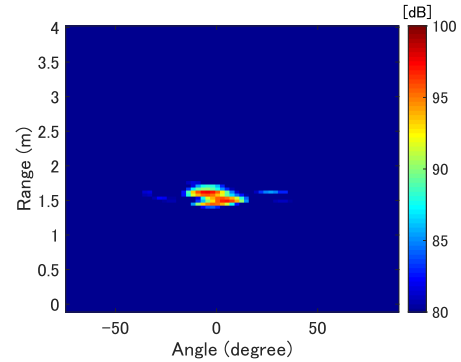


Fig. 3. Example of the radar image $I_p(r, \theta)$.

shows a radar image $I_p(r, \theta)$ that was obtained from data acquired while the patient was asleep, in which we see a set of strong echoes at a range of approximately 1.5 m; this suggests that these echoes arrive from not a single point on the target person's body, but from multiple points. The body displacement waveforms measured at these multiple points were then used to detect apnea and hypopnea events when using the proposed method.

Figs. 4 and 5 show examples of the respiratory displacements measured using the radar system during normal breathing and during apnea and hypopnea events, respectively. In Fig. 4(a)–(d), the respiratory amplitudes remained almost constant within the 60-s epoch. In contrast, in Fig. 5, the apnea and hypopnea respiratory amplitudes were reduced (red lines) when compared with normal respiration (black lines). Fig. 5(a) and (d) shows the obstructive SA (OSA) signs and (b) shows the hypopnea sign. In these three panels, respiratory efforts, i.e., periodic movements similar to those of normal breathing when the amplitude is decreasing, were found. However,

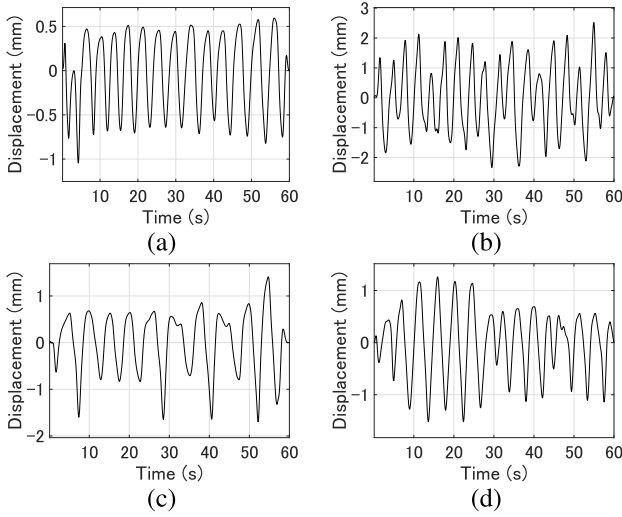


Fig. 4. Examples of respiratory displacements observed during normal breathing. (a) Participant 1, (b) participant 3, (c) participant 4, and (d) participant 5.

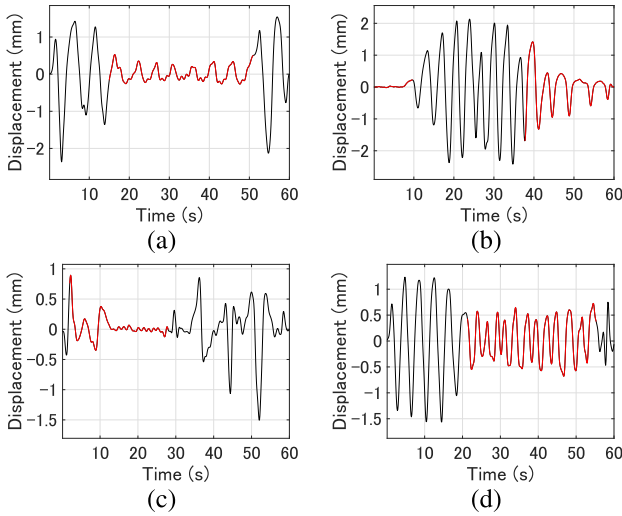


Fig. 5. Examples of respiratory displacements observed when apnea and hypopnea events occur. (a) Participant 1, (b) participant 3, (c) participant 4, and (d) participant 5.

no respiratory effort was observed in Fig. 5(c), showing the central SA (CSA) sign. Therefore, apnea and hypopnea events can be determined visually to some extent from the respiratory displacements measured using radar. We note that all participants' apnea and hypopnea may have included central apnea and hypopnea, nonetheless, most SAS patients have OSA symptoms, and the detection of OSA events is considered important.

Fig. 6 shows examples of the histograms of the respiratory amplitudes (gray bars) and the corresponding probability density functions of the mixed Gaussian distributions that were estimated using the EM algorithm, where each panel (a)–(d) corresponds to (a)–(d) in Fig. 4. In Fig. 6(a) and (b), only one peak is observed, whereas in Fig. 6(c) and (d), we can see two peaks that approximately correspond to μ_1 and μ_2 ($\mu_1 < \mu_2$). This illustrates that there can be two peaks in these characteristics, even when the breathing is normal.

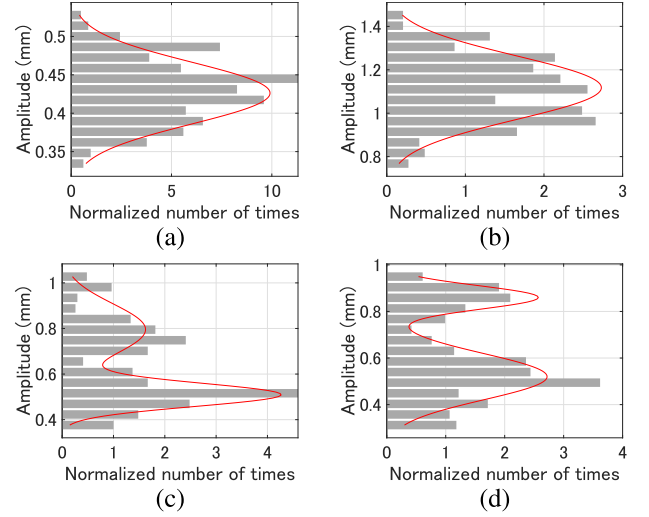


Fig. 6. Probability density functions estimated using the EM algorithm for respiratory amplitudes during normal breathing. (a) Participant 1, (b) participant 3, (c) participant 4, and (d) participant 5.

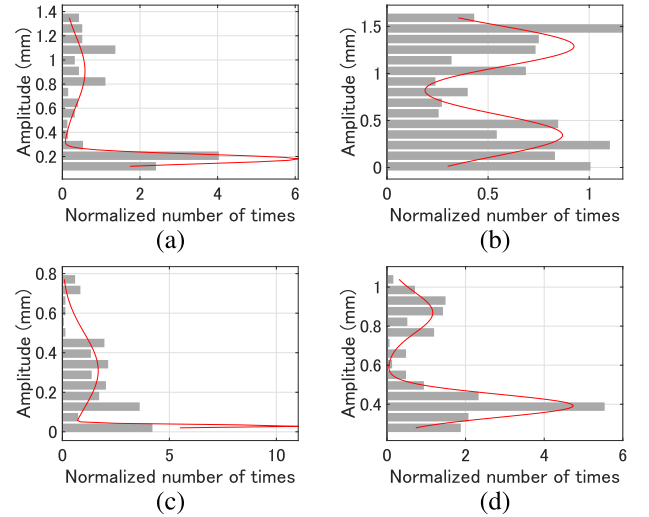


Fig. 7. Probability density functions estimated using the EM algorithm for respiratory amplitudes when apnea and hypopnea events occur. (a) Participant 1, (b) participant 3, (c) participant 4, and (d) participant 5.

Fig. 7 also shows example histograms of the respiratory amplitudes (gray bars) and the corresponding probability density functions when the apnea and hypopnea events occur, corresponding to Fig. 6. In this case, we can see two peaks in all panels and the peak gaps are larger than those observed in Fig. 6 (i.e., μ_1/μ_2 is larger). The proposed method uses these characteristics to detect the apnea and hypopnea events automatically.

C. Accuracy Evaluation of the Proposed Method

This section provides a performance evaluation of the proposed method by comparing it with the conventional ABM. For this performance evaluation, we use the apnea–hypopnea index (AHI), which represents the combined number of apneas and hypopneas that occur per hour during sleep and is used to diagnose the severity of a patient's SAS. In addition, we also evaluate the accuracy of estimation of the number of apnea

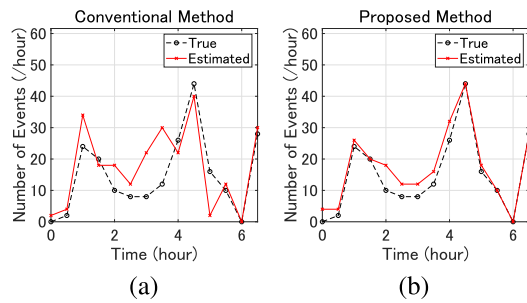


Fig. 8. Number of apnea and hypopnea events estimated at 30-min intervals for participant 1 when using (a) conventional and (b) proposed methods.

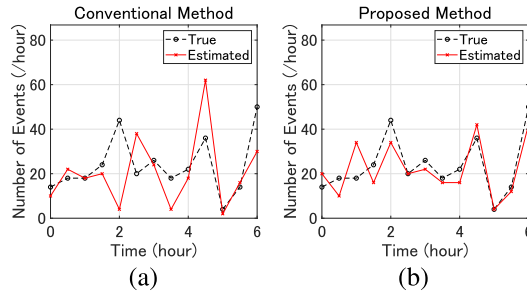


Fig. 9. Number of apnea and hypopnea events estimated at 30-min intervals for participant 2 when using (a) conventional and (b) proposed methods.

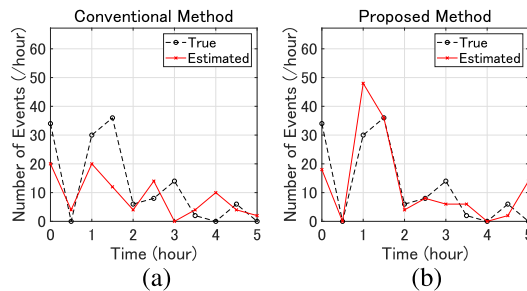


Fig. 10. Number of apnea and hypopnea events estimated at 30-min intervals for participant 3 when using (a) conventional and (b) proposed methods.

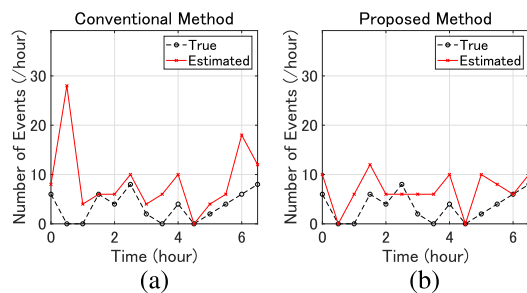


Fig. 11. Number of apnea and hypopnea events estimated at 30-min intervals for participant 4 using (a) conventional and (b) proposed methods.

and hypopnea events per 30 min, which we then convert into the number per hour by simply doubling the number.

Figs. 8–12 show the numbers of apnea and hypopnea events per hour for each participant. In each figure, the red lines in (a) and (b) indicate the estimates from the conventional and proposed methods, respectively. The true numbers of apnea

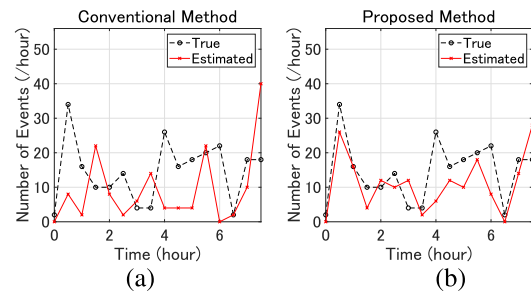


Fig. 12. Number of apnea and hypopnea events estimated at 30-min intervals for participant 5 using (a) conventional and (b) proposed methods.

TABLE II
RMS ERRORS OF ESTIMATED NUMBERS OF APNEA AND HYPOPNEA EVENTS PER HOUR

Patient number	Conventional method	Proposed method
1	8.2	3.5
2	15.9	7.2
3	10.6	8.9
4	8.7	4.4
5	14.0	7.9
Mean	11.5	6.4

TABLE III
AHI ESTIMATED USING THE CONVENTIONAL AND PROPOSED METHODS (TIMES/HOURS)

Patient		Conventional method		Proposed method	
No.	AHI	Estimated AHI	Error	Estimated AHI	Error
1	30.4	35.9	5.5	35.6	5.2
2	51.1	44.5	6.6	47.8	3.3
3	27.2	18.8	8.4	28.4	1.2
4	7.4	18.2	10.8	14.2	6.8
5	30.3	19.1	11.2	23.0	7.3
Mean	-	-	8.5	-	4.8

and hypopnea events, which are plotted as black dashed lines, were obtained from the PSG data and the doctor's diagnosis.

Table II shows the root-mean-square (rms) errors calculated for the estimated numbers of apnea and hypopnea events as shown in Figs. 8–12. For all patients, the rms error of the proposed method was shown to be smaller than that of the conventional method. The rms error averaged over all patients was 11.5 times/h when using the conventional method, whereas the corresponding value when using the proposed method was 6.4 times/h, representing an improvement in accuracy of 1.8 times.

Table III summarizes the AHI values that were estimated using both the conventional and proposed methods. The AHI was estimated to have an average error of 8.5 times/h when using the conventional method and 4.8 times/h when using the proposed method, again resulting in an improvement of 1.8 times. Because the diagnostic criterion for SA is $AHI \geq 5$ times/h, the proposed method estimates the AHI with an accuracy of 4.8 times/h, which reaches the minimum accuracy requirement for diagnosis. These results illustrate the effectiveness of the proposed method for the detection of apnea and hypopnea events in a noncontact manner using a radar system.

V. DISCUSSION

In this study, we have proposed a method for the detection of SA/hypopnea events that can be regarded as decision problems for two hypotheses (i.e., normal breathing and apnea/hypopnea). In decision theory, statistical approaches such as the generalized likelihood ratio test are available. However, rather than adopt an existing statistical method, we have developed a new approach because it is difficult to identify the appropriate statistical model for the radar-measured body displacements caused by respiration that includes apnea and hypopnea, partly because insufficient quantities of radar-measured respiratory displacement data have been collected from patients. In fact, the amplitudes and waveforms of radar-measured respiratory displacement signals are affected strongly by individual differences, and they are also dependent on the type of apnea/hypopnea [i.e., OSA, CSA, and mixed SA (MSA)], the body part to be measured (e.g., the chest, abdomen, front, or back), and the patient's posture (supine, prone, and lateral recumbent positions).

In our problem setting, the EM-based procedure represents the first choice because the EM algorithm is the most commonly used unsupervised approach for the estimation of the model parameters in cases where the statistical distribution is expressed using a Gaussian mixture model. In addition, the use of the EM algorithm allows us to obtain the ratio of the respiratory amplitude for normal breathing to the respiratory amplitude for apnea/hypopnea; this ratio can then be used to detect reduced ventilation due to apnea/hypopnea directly based on the AASM criteria. For these reasons, we selected the EM-based approach rather than use other decision statistics methods for the detection of SA/hypopnea. Despite this, it will be important to investigate the possibility of the application of other statistics-based methods to determine the decision boundary to improve the detection accuracy; however, this aspect will form part of our future studies.

One of the drawbacks of our proposed method is that it is unable to distinguish unwanted limb movements from physiological body displacements, and it is thus suspected that our approach is affected negatively by patient body motion, which can reduce the detection accuracy. Therefore, it will be important to extend our method by including a technique to detect these limb movements and improve the overall detection accuracy in future work. Another important step will be integration of the proposed radar-based method with the PSG system, which has been studied intensively in the literature [31], [32], [33], [34].

VI. CONCLUSION

In this study, we have proposed a novel method for noncontact radar-based SA detection. The proposed method achieves adaptive apnea detection without prior knowledge of the respiratory amplitude of normal breathing. The proposed method uses a histogram of the respiratory amplitude as measured using a radar system, and then detects single or double peaks using the EM algorithm to distinguish the apnea and hypopnea events from normal breathing. To evaluate the performance of our proposed method, we performed experiments using both radar and PSG systems on five patients with SA symptoms.

The experimental results showed that the proposed method estimated the AHI with an accuracy that was 1.8 times higher than that of the conventional method, confirming the effectiveness of the proposed method. In addition, we also demonstrated that the proposed method was able to estimate the AHI with a mean error of only 4.8 times/h, which met the minimum accuracy requirement for use in SAS diagnosis. In conclusion, the proposed method was shown to be effective in using radar to perform noncontact apnea detection.

REFERENCES

- [1] *The AASM Manual for the Scoring of Sleep and Associated Events, Version 3*, American Academy of Sleep Medicine, Darien, IL, USA, Feb. 2023.
- [2] A. V. Benjafield et al., "Estimation of the global prevalence and burden of obstructive sleep apnoea: A literature-based analysis," *Lancet Respiratory Med.*, vol. 7, no. 8, pp. 687–698, Aug. 2019.
- [3] M. L. Jackson, M. E. Howard, and M. Barnes, "Cognition and daytime functioning in sleep-related breathing disorders," *Prog. Brain Res.*, vol. 190, pp. 53–68, Jan. 2011.
- [4] R. Budhiraja, P. Budhiraja, and S. F. Quan, "Sleep-disordered breathing and cardiovascular disorders," *Respiratory Care*, vol. 55, no. 10, pp. 1322–1332, Oct. 2010.
- [5] K. A. Franklin and E. Lindberg, "Obstructive sleep apnea is a common disorder in the population—A review on the epidemiology of sleep apnea," *J. Thoracic Disease*, vol. 7, no. 8, pp. 1311–1322, Aug. 2015.
- [6] V. K. Kapur et al., "Clinical practice guideline for diagnostic testing for adult obstructive sleep apnea: An American academy of sleep medicine clinical practice guideline," *J. Clin. Sleep Med.*, vol. 13, no. 3, pp. 479–504, Mar. 2017.
- [7] A. Q. Javaid, C. M. Noble, R. Rosenberg, and M. A. Weitnauer, "Towards sleep apnea screening with an under-the-mattress IR-UWB radar using machine learning," in *Proc. IEEE 14th Int. Conf. Mach. Learn. Appl. (ICMLA)*, Dec. 2015, pp. 837–842.
- [8] S. M. M. Islam, A. Rahman, E. Yavari, M. Baboli, O. Boric-Lubecke, and V. M. Lubecke, "Identity authentication of OSA patients using microwave Doppler radar and machine learning classifiers," in *Proc. IEEE Radio Wireless Symp. (RWS)*, Jan. 2020, pp. 251–254.
- [9] H. B. Kwon et al., "Hybrid CNN-LSTM network for real-time apnea-hypopnea event detection based on IR-UWB radar," *IEEE Access*, vol. 10, pp. 17556–17564, 2022.
- [10] T. Koda, T. Sakamoto, S. Okumura, H. Taki, S. Hamada, and K. Chin, "Radar-based automatic detection of sleep apnea using support vector machine," in *Proc. Int. Symp. Antennas Propag. (ISAP)*, Jan. 2021, pp. 841–842.
- [11] F. Snigdha, S. M. M. Islam, O. Boric-Lubecke, and V. Lubecke, "Obstructive sleep apnea (OSA) events classification by effective radar cross section (ERCS) method using microwave Doppler radar and machine learning classifier," in *IEEE MTT-S Int. Microw. Symp. Dig.*, Dec. 2020, pp. 1–3, doi: 10.1109/IMBIO47321.2020.9385028.
- [12] K. Fukuyama, O. Sugiyama, K. Chin, S. Satou, S. Matsumoto, and M. Muto, "Identification of respiratory sounds collected from microphones embedded in mobile phones," *Adv. Biomed. Eng.*, vol. 11, pp. 58–67, Jan. 2022.
- [13] L. Anishchenko, L. Korostovtseva, M. Bochkarev, and Y. Sviryaev, "Sleep breathing disorders detection with bioradar using a long short-term memory network," in *Proc. XXXIIIrd Gen. Assem. Sci. Symp. Int. Union Radio Sci.*, Aug. 2020, pp. 1–4.
- [14] C. Yang, X. Wang, and S. Mao, "Unsupervised detection of apnea using commodity RFID tags with a recurrent variational autoencoder," *IEEE Access*, vol. 7, pp. 67526–67538, 2019.
- [15] J. Xiong, J. Jiang, H. Hong, C. Gu, Y. Li, and X. Zhu, "Sleep apnea detection with Doppler radar based on residual comparison method," in *Proc. Int. Appl. Comput. Electromagn. Soc. Symp. (ACES)*, Aug. 2017, pp. 1–2.
- [16] J. Xiong, J. Jiang, H. Hong, C. Gu, Y. Li, and X. Zhu, "CW radar based OSA detection solution with residual comparison method," in *IEEE MTT-S Int. Microw. Symp. Dig.*, vol. 1, May 2019, pp. 1–3.
- [17] M. Baboli, A. Singh, B. Soll, O. Boric-Lubecke, and V. M. Lubecke, "Wireless sleep apnea detection using continuous wave quadrature Doppler radar," *IEEE Sensors J.*, vol. 20, no. 1, pp. 538–545, Jan. 2020.

- [18] N. Du, K. Liu, L. Ge, and J. Zhang, "ApneaRadar: A 24 GHz radar-based contactless sleep apnea detection system," in *Proc. 2nd Int. Conf. Frontiers Sensors Technol. (ICFST)*, Apr. 2017, pp. 372–376.
- [19] M. Kagawa, K. Ueki, H. Tojima, and T. Matsui, "Noncontact screening system with two microwave radars for the diagnosis of sleep apnea-hypopnea syndrome," in *Proc. 35th Annu. Int. Conf. IEEE Eng. Med. Biol. Soc. (EMBC)*, Jul. 2013, pp. 2052–2055.
- [20] M. Kagawa, H. Tojima, and T. Matsui, "Non-contact screening system for sleep apnea-hypopnea syndrome using the time-varying baseline of radar amplitudes," in *Proc. IEEE Healthcare Innov. Conf. (HIC)*, Oct. 2014, pp. 99–102.
- [21] F. Qi, C. Li, S. Wang, H. Zhang, J. Wang, and G. Lu, "Contact-free detection of obstructive sleep apnea based on wavelet information entropy spectrum using bio-radar," *Entropy*, vol. 18, no. 8, p. 306, Aug. 2016.
- [22] F. Qi, J. Wang, and A. E. Fathy, "Automatic and accurate non-contact obstructive sleep apnea detection using wavelet information entropy spectrum," in *Proc. USNC-URSI Radio Sci. Meeting (Joint AP-S Symposium)*, Jul. 2019, pp. 55–56.
- [23] R. N. Khushaba, J. Armitstead, and K. Schindhelm, "Monitoring of nocturnal central sleep apnea in heart failure patients using noncontact respiratory differences," in *Proc. 39th Annu. Int. Conf. IEEE Eng. Med. Biol. Soc. (EMBC)*, Jul. 2017, pp. 1534–1538.
- [24] G. Fedele, E. Pittella, S. Pisa, M. Cavagnaro, R. Canali, and M. Biagi, "Sleep-apnea detection with UWB active sensors," in *Proc. IEEE Int. Conf. Ubiquitous Wireless Broadband (ICUBW)*, Oct. 2015, pp. 1–5.
- [25] S. Kang et al., "Non-contact diagnosis of obstructive sleep apnea using impulse-radio ultra-wideband radar," *Sci. Rep.*, vol. 10, p. 5261, Mar. 2020.
- [26] T. Koda, T. Sakamoto, S. Okumura, and H. Taki, "Noncontact respiratory measurement for multiple people at arbitrary locations using array radar and respiratory-space clustering," *IEEE Access*, vol. 9, pp. 106895–106906, 2021.
- [27] W. R. Ruehland et al., "The new AASM criteria for scoring hypopneas: Impact on the apnea hypopnea index," *sleep*, vol. 32, no. 2, pp. 150–157, Feb. 2009.
- [28] R. B. Berry et al., "Rules for scoring respiratory events in sleep: Update of the 2007 AASM manual for the scoring of sleep and associated events," *J. Clin. Sleep Med.*, vol. 8, no. 5, pp. 597–619, Oct. 2012.
- [29] M. M. Troester, S. F. Quan, and R. B. Berry, *The AASM Manual for the Scoring of Sleep and Associated Events; Terminology and Technical Specification. Version3*, American Academy of Sleep Medicine, Darien, IL, USA, 2023.
- [30] T. Leppänen et al., "Length of individual apnea events is increased by supine position and modulated by severity of obstructive sleep apnea," *Sleep Disorders*, vol. 2016, no.1, Mar. 2016, Art. no. 9645347.
- [31] A. Singh et al., "Considerations for integration of a physiological radar monitoring system with gold standard clinical sleep monitoring systems," in *Proc. 35th Annu. Int. Conf. IEEE Eng. Med. Biol. Soc. (EMBC)*, Osaka, Japan, Jul. 2013, pp. 2120–2123, doi: [10.1109/EMBC.2013.6609952](https://doi.org/10.1109/EMBC.2013.6609952).
- [32] M. Baboli, A. Singh, B. Soll, O. Boric-Lubecke, and V. M. Lubecke, "Good night: Sleep monitoring using a physiological radar monitoring system integrated with a polysomnography system," *IEEE Microw. Mag.*, vol. 16, no. 6, pp. 34–41, Jul. 2015, doi: [10.1109/MMM.2015.2419771](https://doi.org/10.1109/MMM.2015.2419771).
- [33] M. Baboli, "Physiological radar system for diagnosing sleep disorders," Ph.D. dissertation, Dept. Elect. Eng., Univ. Hawaii, Honolulu, HI, USA, 2014.
- [34] M. Baboli, B. Soll, O. Boric-Lubecke, and V. Lubecke, "Doppler radar for sleep medicine," in *Proc. Asia-Pacific Microw. Conf.*, Sendai, Japan, Nov. 2014, pp. 953–955.



Takato Koda received the B.E. degree in electrical and electronic engineering from Kyoto University, Kyoto, Japan, in 2020, and the M.E. degree in electrical engineering from the Graduate School of Engineering, Kyoto University, in 2022.



Shigeaki Okumura received the B.E. degree in electrical engineering from Kyoto University, Kyoto, Japan, in 2013, and the M.I. and Ph.D. degrees in communications and computer engineering from the Graduate School of Informatics, Kyoto University, in 2015 and 2018, respectively.

He has been with MaRI Company Ltd., Kyoto, since 2019. His research interests include radar and audio signal processing and the noncontact measurement of vital signs.



Hirofumi Taki (Member, IEEE) received the M.D. and Ph.D. degrees in informatics from Kyoto University, Kyoto, Japan, in 2000 and 2007, respectively.

He was an Assistant Professor with the Graduate School of Informatics, Kyoto University, and also an Associate Professor with the Graduate School of Biomedical Engineering, Tohoku University, Sendai, Japan. He founded MaRI Company Ltd., Kyoto, in 2017, where he has been the CEO ever since. His research

interests include digital signal processing in measurement of biological information.



Satoshi Hamada received the Ph.D. degree in respiratory medicine from the Graduate School of Medicine, Kyoto University, Kyoto, Japan, in 2016.

He is currently an Assistant Professor with the Department of Advanced Medicine for Respiratory Failure, Graduate School of Medicine, Kyoto University Hospital, Kyoto.



Hironobu Sunadome received the Ph.D. degree in respiratory medicine from the Graduate School of Medicine, Kyoto University, Kyoto, Japan, in 2021.

He is currently an Assistant Professor with the Department of Respiratory Care and Sleep Control Medicine, Graduate School of Medicine, Kyoto University. His subspecialty is respiratory medicine, allergic medicine, and sleep breathing medicine.



Susumu Sato received the Ph.D. degree in respiratory medicine from the Graduate School of Medicine, Kyoto University, Kyoto, Japan, in 2004.

He is currently an Associate Professor with the Department of Respiratory Care and Sleep Control Medicine, Graduate School of Medicine, Kyoto University, Kyoto, Japan. He is also the Head of the Section of the Sleep Laboratory, Kyoto University Hospital, Kyoto. His subspecialty is respiratory medicine. His current research fields are respiratory medicine, respiratory mechanics, biomedical engineering, and image analysis, including outcome research.

Dr. Sato is a Deputy Head of the Assembly of Respiratory Structure and Function of Asia-Pacific Society of Respiriology (APSR).



Kazuo Chin received the M.D and Ph.D. degrees in internal medicine from the Graduate School of Medicine, Kyoto University, Kyoto, Japan, in 1981 and 1990, respectively.

He was a Program Specific Professor with the Department of Respiratory Care and Sleep Control Medicine, Graduate School of Medicine, Kyoto University, from 2008 to 2021. He is currently a specially-appointed Professor with the Department of Sleep Medicine and Respiratory Care, Division of Sleep Medicine, Nihon University of Medicine, Tokyo, Japan. At the same time, he also works part-time with the Department of Human Disease Genomics, Center for Genomic Medicine, Graduate School of Medicine, Kyoto University. His research interests are respiratory care and sleep medicine, including sleep disordered breathing.



Takuya Sakamoto (Senior Member, IEEE) received the B.E. degree in electrical and electronic engineering from Kyoto University, Kyoto, Japan, in 2000, and the M.I. and Ph.D. degrees in communications and computer engineering from the Graduate School of Informatics, Kyoto University, in 2002 and 2005, respectively.

From 2006 to 2015, he was an Assistant Professor with the Graduate School of Informatics, Kyoto University. From 2011 to 2013, he was a Visiting Researcher with Delft University of Technology, Delft, The Netherlands. From 2015 to 2019, he was an Associate Professor at the Graduate School of Engineering, University of Hyogo, Himeji, Japan. In 2017, he joined the University of Hawaii at Manoa, Honolulu, HI, USA, as a Visiting Scholar. From 2019 to 2022, he was an Associate Professor with the Graduate School of Engineering, Kyoto University. From 2018 to 2022, he was also a PRESTO Researcher at the Japan Science and Technology Agency, Kawaguchi, Japan. Since 2022, he has been a Professor at the Graduate School of Engineering, Kyoto University. His current research interests lie in wireless human sensing, radar signal processing, and radar measurement of physiological signals.

Prof. Sakamoto was a recipient of the Best Paper Award from the International Symposium on Antennas and Propagation (ISAP) in 2004; the Young Researcher's Award from the Information and Communication Engineers of Japan (IEICE) in 2007; the Best Presentation Award from the Institute of Electrical Engineers of Japan in 2007; the Best Paper Award from the ISAP in 2012; the Achievement Award from the IEICE Communications Society in 2015, 2018, and 2023; the Achievement Award from the IEICE Electronics Society in 2019; the Masao Horiba Award in 2016; the Best Presentation Award from the IEICE Technical Committee on Electronics Simulation Technology in 2022; the Telecom System Technology Award from the Telecommunications Advancement Foundation in 2022; and the Best Paper Award from the IEICE Communication Society in 2007 and 2023.